ADVANCED FUNCTIONAL MATERIALS
www.afm-journal.de

Materials Views
www.MaterialsViews.com

N,7,7-Tricyanoquinomethanimine (TCQMI) Based Organic Magnetic Materials

*Jordan L. Arthur, Saul H. Lapidus, Curtis E. Moore, Arnold L. Rheingold, Peter W. Stephens, and Joel S. Miller**

This manuscript is dedicated to the memory of Professor Alan G. MacDiarmid

The synthesis and characterization of a new family of magnetic materials based on the electron accepting cyanocarbon *N*,7,7-tricyanoquinomethanimine, TCQMI, its radical anion [TCQMI], and its σ-dimer, σ-$[TCQMI]_2^{2-}$, are reported. $[Fe^{III}Cp^*_2][TCQMI]$ (where Cp^* is pentamethylcyclopentadienide) forms parallel chains of alternating $[TCQMI]^{\bullet-}$ and $[FeCp^*_2]^{\bullet+}$ and magnetically orders at 3.4 K as a weak ferromagnet. $M[TCQMI]_2 \bullet zCH_2Cl_2$ (M = V, Fe) are amorphous solids with $[TCQMI]^{\bullet-}$ coordinated to metal centers through the nitrile groups. The Fe compound magnetically orders as a weak ferromagnet at ≈4 K, whereas the V compound shows no evidence of magnetic ordering. $\{[Mn^{III}TPP]^+\}_2[TCQMI]_2^{2-}$ (TPP = tetraphenylporphyrin) results from the reaction of TCQMI with $Mn^{II}TPP(py)$ due to the formation of the $[TCQMI]_2^{2-}$ σ-dimer in situ, and is a weak ferromagnet below 3.7 K. The lack of magnetic ordering in $V[TCQMI]_2 \bullet zCH_2Cl_2$ is not currently understood, and is in strong contrast to $V[TCNE]_2 \bullet zCH_2Cl_2$, which magnetically orders above room temperature.

1. Introduction

Molecule-based electronics have been of increasing interest since the discovery of organic-based metals, particularly with the discovery of [TTF][TCNQ] (TTF = tetrathiafulvalene; TCNQ = 7,7,8,8-tetracyano-*p*-quinodimethane), which forms segregated chains of alternating cationic TTF and anionic TCNQ.[1] The first magnetically ordered organic-based material was observed for $[FeCp^*_2]^{\bullet+}[TCNQ]^{\bullet-}$ (Cp^* = pentamethylcyclopentadienide), which exhibited metamagnetic behavior.[2] Above a 1300 Oe applied critical field, H_c, it exhibited ferromagnetic-like behavior with a magnetic ordering temperature, T_c, of 2.5 K.[2a,3] The structure of $[FeCp^*_2]^{\bullet+}[TCNQ]^{\bullet-}$ consists of alternating chains of $[FeCp^*_2]^{\bullet+}$ cations and $[TCNQ]^{\bullet-}$ anions. This discovery led to the design and synthesis of $[FeCp^*_2]^{\bullet+}[TCNE]^{\bullet-}$ (TCNE = tetracyanoethylene), which is a bulk ferromagnet (T_c = 4.8 K), and extended the use of organic radical carriers in forming magnetically ordered materials worldwide.[4] Many organic-based magnets possess cyanocarbon acceptors, including functionalized TCNQ derivatives,[5] TCNE,[6] *N*,*N*′-dicyanoquinone diimine (DCNQI) derivatives,[7] hexacyanobutadiene (HCBD),[8] and hexacyanotrimethylenecyclopropane (HCTMCP).[9] Each of these acceptors is readily reduced to a stable radical anion. In addition, the ability of the nitrile groups to coordinate to metal ions has enabled the formation of extended network structures. 0-, 1-, 2-, and 3D lattices have been reported that display interesting and important magnetic behaviors.[4,10,11]

Several magnetic coordination compounds based on reduced of TCNE and TCNQ have been structurally characterized. An octahedrally coordinated metal ion bonds to six nitriles in a 2:3 M:$[TCNE]^{\bullet-}$ ratio for the 171-K ferrimagnet $Mn^{II}[TCNE]_{3/2}(I_3)_{1/2} \bullet z$THF.[12] Several materials based on 2D networks of octahedral metals equatorially bonded to μ_4-$[TCNE]^{\bullet-}$, with two axial bonds of magnetically inert moieties to the metal ion, have been described, with magnetic ordering temperatures in the range 68 to 171 K.[13] Materials of composition $M[TCNQ]_2$ (M = Mn, Fe, Co, Ni) have been described with ordering temperatures between 7 and 44 K, but they have not been structurally characterized.[14] Tetrahedrally coordinated Ag[TCNQ] and Cu[TCNQ] do not magnetically order; however, this is due to the lack of spin on the M^I sites.[15]

To date, all of the cyanocarbon-based magnetic materials have been symmetric, and possess an even number of nitrile groups. The paucity of magnetic systems designed with asymmetric cyanocarbon acceptors has led us to study the asymmetric

J. L. Arthur, Prof. J. S. Miller
Department of Chemistry
University of Utah
Salt Lake City, UT 84112-0850, USA
E-mail: jsmiller@chem.utah.edu
S. H. Lapidus, Prof. P. W. Stephens
Department of Physics and Astronomy
Stony Brook University
Stony Brook, NY 11794, USA
Dr. C. E. Moore, Prof. A. L. Rheingold
Department of Chemistry
University of California
San Diego, La Jolla, CA 92093-0358, USA
Prof. P. W. Stephens
Photon Sciences Directorate
Brookhaven National Laboratory
Upton, NY 11973, USA

DOI: 10.1002/adfm.201101937

N,7,7-tricyanoquinodimethanimine (TCQMI)[16] and its ability to form new organic-based magnetic materials. Unlike both TCNE and TCNQ, TCQMI has three nitriles; thus, in principle, two TCQMI's could fully satisfy the coordination environment in a 1:2 ratio of M^{II}:TCQMI. Additionally, due to the presence of the -NCN- moiety, a shorter three-atom M-NCN-M linkage, with respect to the more prevalent five atom M-NCCCN-M, could provide a stronger coupling enabling a higher T_c, as observed for $M[N(CN)_2]$ magnetic materials.[17]

TCQMI has been previously reported[16a,c] and has two reversible one-electron reductions at 0.20 and –0.47 volts (V) versus a saturated calomel electrode (SCE), in good agreement with literature values.[16a] The former is comparable to the first reduction potentials of both TCNE (0.24 V vs. SCE) and TCNQ (0.22 V vs. SCE).[18] This indicates that $[TCQMI]^{\bullet-}$ should be isolatable and suitable for forming molecule-based magnetic materials. Hence, the reaction of TCQMI with $FeCp^*_2$, $Fe(CO)_5$, $V(CO)_6$, and MnTPP were pursued to identify new organic-based magnets.

Here, we report the structures of TCQMI and $[TCQMI]^{\bullet-}$ as well as the magnetic behavior of molecule-based materials incorporating this cyanocarbon ligand. The σ-dimer, $[TCQMI]_2^{2-}$, present in $\{[Mn^{III}TPP]\}_2[TCQMI]_2$ was discussed previously,[19] and herein we report additional information on that material.

2. Experimental Section

2.1. Synthesis

The solvents used in the generation of organic radicals were dried, distilled, and deoxygenated prior to use. Steps generating organic radicals were conducted under an inert N_2 atmosphere in a DriLab glove box (<1 ppm O_2). Cyclohexane-1,4-dione (Alfa Aesar), *p*-toluenesulfonic acid (Lancaster Chemical), 1,4-butanediol (Sigma), acetic acid (EMD), malononitrile (Arcos), bis(trimethylsilyl)carbodiimide (Petrarch Systems, Inc.), and decamethylferrocene (Arcos Organics) were used without further purification. $TiCl_4$ (Janssen Chimica) was distilled under vacuum and stored under a dry N_2 atmosphere. $Fe(CO)_5$ was purchased from Fisher Scientific and freeze-pump-thawed over several cycles to deoxygenate the compound. $V(CO)_6$ was synthesized from $[NEt_4][V(CO)_6]$ following a literature procedure.[20] MnO_2 was prepared freshly before use according to the methods of Attenburrow et al.,[21] with the substitution of $MnCl_2{\bullet}4H_2O$ for $MnSO_4{\bullet}4H_2O$.

TCQMI was synthesized through the combination of two methods.[16b],c] First, *p*-dicyanomethylenebenzoquinone (DCMBQ) was formed following a modification of a route described by Hyatt.[16b] Modifications included isolating the mono-ketal from unreacted starting material by serial separation in a 1:4 solution of acetonitrile and hexanes. 1,4-cyclohexanedione dissolved easily into the acetonitrile layer while the desired oily mono-ketal, 1,2-dioxaspiro[5.6]dodecan-3-one, remained in the hexane layer. Additional modifications to the preparation included repeating the deprotection of the mono-ketal intermediate to increase the purity of the resulting ketone. Also, the MnO_2 used in the reduction to DCMBQ was always prepared fresh and used after drying in an oven at 105 °C.[21] Despite these precautions, the yield of 9% was always much lower than the 45% reported previously.[16b]

TCQMI was synthesized using a modification to the preparation reported by Iwatsuki and co-workers.[16c] Purification was achieved by recrystallization from a 1:1 solution of benzene and hexanes leading to red-orange crystals after five days that were suitable for single crystal X-ray diffraction. [Yield: 81.9 mg (71%) (from DCMBQ)]. IR (KBr; cm^{-1}): 2230 s (ν_{CN}), 2169 s (ν_{CN}), 1548 s, 864 m; NMR ($CDCl_3$) δ: 7.69 (dd, 1H), 7.63 (dd, 1H), 7.40 (dd, 1H), 7.19 (dd, 1H).

$[Fe^{III}Cp^*_2]^{+}[TCQMI]^{\bullet-}$ was synthesized by adding one equivalent of TCQMI (16.6 mg, 0.0.921 mmol) dissolved in 20 mL MeCN dropwise to an equivalent of $Fe^{II}Cp^*_2$ (25.3 mg, 0.0774 mmol) dissolved in 20 mL MeCN in a glove box. This resulted in an immediate color change to a dark green/blue. The reaction was stirred for 2 days in the glove box and no further color change was observed and no precipitate was formed. The solution was then placed in a freezer in a glove box for 4 days, during which time clusters of a dark green clay-like powder precipitated [Yield: 31 mg (79%)]. Crystals suitable for single crystal X-ray diffraction could not be obtained, and the structure was determined with the use of synchrotron powder X-ray diffraction data. IR (KBr; cm^{-1}): ν_{CN}, 2185 m, 2169 m, 2150 m, 2131 m, 2098 m.

Attempts were made to grow crystals in order to provide a purer sample. The reaction was repeated in CH_2Cl_2 and solid was seen to precipitate out of the solution upon standing in a freezer for 4 days. The solid appeared somewhat clay-like but was the same color as the solid taken from the previous reaction. Interestingly, when the solid was collected and dried, the resulting IR spectrum proved to be nearly identical to that seen from the taking the solution to dryness.

$Fe[TCQMI]_2{\bullet}zCH_2Cl_2$ was prepared by dissolving $Fe(CO)_5$ (53 mg, 0.271 mmol) and TCQMI (96.5 mg, 0.536 mmol) each in 15 mL CH_2Cl_2. The $Fe(CO)_5$ solution (pale yellow) was added dropwise to the orange TCQMI solution with no immediate color change. The color slowly darkened to green/black over the course of 4 h, with a precipitate forming after several hours. The solution was left to stir for 5 days in a glove box at room temperature, after which time a dark green precipitate was collected by filtration, washed with hexanes until the filtrate was colorless, and then placed in a drying tube for 4 h. [Yield: 102 mg (91%)]. IR (KBr; cm^{-1}): ν_{CN} 2245 w, 2173 s, 2116 s. Anal. calcd (obsd) for $Fe[TCQMI]_2{\bullet}zCH_2Cl_2$, $z = 0.38$: C 54.58 (54.43), H 1.97 (1.97), N 24.99 (24.89), Cl 6.01 (6.30), Fe 12.45 (12.41). The loss of CH_2Cl_2 is facile and thus there is poor baseline; nonetheless a 6.8% weight loss occurs below 242 °C in the TGA trace that is attributed to the CH_2Cl_2 loss and corresponds to z = 0.36.

$V[TCQMI]_2{\bullet}zCH_2Cl_2$ was prepared by the procedure outlined for the synthesis of $V[TCNQ]_2$.[22] TCQMI (82.3 mg, 0.457 mmol) was dissolved in 15 mL of CH_2Cl_2 and $V(CO)_6$ (51.3 g, 0.228 mmol) was dissolved in 5 mL of CH_2Cl_2. After filtering each solution, the solution of $V(CO)_6$ was dropwise added to the solution of TCQMI with stirring. Immediately the TCQMI solution turned black and a black precipitate formed. After the addition of a few drops, the solution bubbled due to carbon monoxide liberation. After the addition was completed, the reaction was stirred for a 15 min with occasional venting

and then stirred overnight. The next day, the dark precipitate was filtered off, washed with CH_2Cl_2, and dried under vacuum at room temperature, yielding a dark black solid. [Yield: 95 mg (99%)]. IR (KBr; cm^{-1}): ν_{CN} 2250 sh, 2086 s. Anal. calcd (obsd) for $V[TCQMI]_2 \bullet zCH_2Cl_2$, $z = 0.10$ calculated from the thermogravimetric analysis (TGA) data.

$\{[Mn^{III}TPP]^+\}_2[TCQMI]_2^{2-}$ was synthesized as described previously.[19] (Yield = 11%). IR (KBr; cm^{-1}): 2188 w, 2140 sh, 2106 br.

2.2. Physical Methods

IR spectra were acquired using a Bruker Tensor 37 spectrometer from KBr pellets (±1 cm^{-1}). NMR (^1H and ^{13}C) were conducted on a Varian Unity 300 spectrometer equipped with a Nalorac Quad-probe ($^1H/^{19}F$, $^{13}C/^{31}P$) direct probe. UV-vis studies were conducted using quartz cuvettes on a Hitachi u-4100 spectrometer. Magnetic susceptibility data were measured at 1 kOe between 2 and 300 K on a Quantum Design MPMS-5XL 5 T SQUID magnetometer equipped with a reciprocating sample measurement system as previously described.[23] The samples were placed in the magnetometer and the magnetic field was removed by oscillating the field until it had reached zero. The magnetometer was then cooled, the field was applied, and data were recorded upon warming. Magnetic studies were conducted in a gelatin capsule. AC susceptibilities were recorded at 33, 100, and 1000 Hz. In addition to correcting for the diamagnetic contribution from the sample holder, the core diamagnetic corrections of –270, –181, and -167×10^{-6} emu mol^{-1} were used for $[FeCp^*_2][TCQMI]$, $Fe[TCQMI]_2$, and $V[TCQMI]_2$, respectively. Instrumental oxygen contamination is responsible for an interruption of the data from 30–60 K, though an attempt to minimize the disruption has been made by subtracting out the oxygen moment. Iron impurities of 39 and 20 ppm were estimated for $[FeCp^*_2][TCQMI]$ and $Fe[TCQMI]_2$, respectively, from fits to Honda plots. Reduction potentials were measured on a Bioanalytical Systems, Inc. Epsilon EC using a $Ag/AgNO_3$ electrode with $[NBu_4][PF_6]$ as the supporting electrolyte and ferrocene ($FeCp_2$) as the reference. Reduction potentials were corrected to reflect V versus SCE . TGA was conducted on a TA Instruments Q500 located in a Vacuum Atmospheres DriLab under inert atmosphere (N_2) to avoid O_2/H_2O degradation of the samples. Samples were loaded in an aluminum pan, heated for 10 min at 20°C before ramping from 20 to 600 °C at 5.00 °C min^{-1} under a continuous N_2 purge of 10 mL min^{-1}. Elemental analysis (EA) was performed by Desert Analytics, Tucson, AZ.

2.3. X-Ray Structure Determination

The crystal structure of TCQMI was determined on a Nonius KappaCCD diffractometer equipped with Mo Kα radiation. All the reflections were merged and only those for which $I_o > 2\sigma(I)$ were included in the refinement, where $\sigma(F_o)^2$ is the standard deviation based on counting statistics. The data for TCQMI were integrated using the Bruker SAINT software program.[24] The structure was solved by a combination of direct methods and heavy atom methods. Patterson methods and the refinement by full-matrix least-squares methods using SHELXL-97 were used for the structures of TCQMI. All the non-hydrogen atoms were refined with anisotropic displacement coefficients. Hydrogen atoms were assigned isotropic displacements $U(H) = 1.2U(C)$, and their coordinates were allowed to ride on their respective carbons using SHELXL97.[25]

High-resolution powder X-ray diffraction (XRPD) measurements of $[FeCp^*_2][TCQMI]$ were collected on the X16C beam line at the National Synchrotron Light Source, Brookhaven National Laboratory. A Si(111) channel-cut monochromator selected a parallel 0.699975-Å incident beam. The diffracted X-rays were analyzed by a Ge(111) crystal and detected using a NaI scintillation counter. The capillary was spun at several Hz during data collection to improve particle statistics. The powder diffraction pattern was indexed and a tentative space group of $P2_1$ was assigned.[26] Simulated annealing was used to determine the structure of $[FeCp^*_2][TCQMI]$.[27] After obtaining an acceptable agreement between observed and calculated patterns, Rietveld refinements were performed in order to improve the structure. Hydrogens were placed in idealized positions. Bonds of similar nature (e.g., nominally single C–C bonds in the TCQMI ring, separate from nominally double bonds) were restrained to be equal and individually refined. Likewise, angles of a similar nature (e.g., C–C–C and C–C=C angles in the TCQMI ring) were restrained to be equal and refined. The Cp^* rings were restrained to be parallel with one another, but allowed to rotate about their common axis.

3. Results and Discussion

TCQMI exhibited two sharp ν_{CN} absorptions at 2230 and 2169 cm^{-1}. The higher energy peak compares well with TCNQ with ν_{CN} bands at around 2220 cm^{-1},[22] while the lower energy band is attributed to the C≡N cyanimine stretch. Interestingly, there was no C=N stretch in the ≈1700 cm^{-1} region typical of imines. The peak at 1548 cm^{-1} (m) is consistent with the spectrum reported by Itoh and co-workers,[16c] but it is more likely attributed to the C=C stretch in the ring.

Reduction of TCQMI was sought through reactions with $Fe^{II}Cp^*_2$, $Fe(CO)_5$, $V(CO)_6$, and Mn(TPP)(py) (H_2TPP = tetraphenylporphyrin; py = pyridine) with the goal of forming new organic-based magnets and determining the structure and behavior of reduced TCQMI. Reaction of TCQMI with $Fe^{II}Cp^*_2$ in MeCN formed a dark green powder that exhibited a weak ν_{CN} absorption at 2241 cm^{-1}, and several medium ν_{CN} bands at 2185, 2169, 2150, 2131, and 2098 cm^{-1} and a shoulder at 2106 cm^{-1}. The bands were generally shifted to lower wavenumbers, consistent with that observed for the reduction of TCNQ[2c] and TCNE.[4] The six peaks is in contrast to the three inequivalent nitriles in the crystal structure (vide infra). Evidence of additional phases or unreacted starting material is not observed; thus, the origin of the extra IR lines is not currently understood. Hence, based on the IR spectrum the reaction of TCQMI with $Fe^{II}Cp^*_2$ forms $[Fe^{III}Cp^*_2]^+[TCQMI]^{\bullet-}$.

The reactions of $Fe(CO)_5$ and $V(CO)_6$ with TCQMI in CH_2Cl_2 led to precipitates with IR ν_{CN} peaks at 2245, 2173, and 2116 cm^{-1} for the former, and 2250 (sh) and 2086 (s) cm^{-1} for the latter. The two lower frequency peaks, like that observed for the

reaction with $FeCp^*_2$, were consistent with a radical anion, as they were shifted to lower energy in comparison to TCQMI°. The peak at 2245 cm^{-1} was unexpected from radical formation, as it was higher in energy. A possible explanation could be that the higher ν_{CN} band may result from a nitrile bridging between metal centers, as this has been seen to cause a comparable shift in nitrile stretches in Prussian Blues analogues.[28] High-energy peaks are also observed in the spectra of $Fe[TCNQ]_2 \cdot zCH_2Cl_2$ (2194 cm^{-1}).[29] Both dark green materials were analyzed by powder diffraction in hopes of determining the structure but did not produce usable patterns.

The IR spectra of the products from the reaction of $V(CO)_6$ and $Fe(CO)_5$ with TCQMI are similar to that seen from the reaction of TCQMI with Mn(TPP)(py). Evidence for the reduction of TCQMI° by MnTPP could be seen by the ν_{CN} IR (KBr) absorptions red-shifting from 2230 and 2169 cm^{-1} for TCQMI° to 2188 and 2106 cm^{-1}. In all compounds, the ν_{CN} absorptions were much broader than that of the neutral TCQMI. This lends further support to the characterization of the compound as $[TCQMI]^{\bullet-}$ to M^{II} centers as it has been observed that coordinating cyano-acceptors, specifically *N,N′*-dicyanoquinone diimines, typically showed broad ν_{CN} stretches.[30] Note that despite the large number of ν_{CN} stretches, the stretches from $[Fe^{III}Cp^*_2]^{\bullet+}[TCQMI]^{\bullet-}$ remain relatively sharp in comparison to $Fe[TCQMI]_2$. This is consistent with $[TCQMI]^{\bullet-}$ forming non-bonding chains with $[FeCp^*_2]^+$, but not coordinating to the Fe^{III} center.

3.1. Structure

The structure of TCQMI (**Figure 1**) was previously unknown, although structures of tri- and tetramethyl-substituted TCQMI analogs (Me_3TCQMI and Me_4TCQMI, respectively) have been previously reported.[16a] The structure of TCQMI•1/2(benzene) is consistent with expectations; within ring C–C bonds of 1.452 Å and C=C bond lengths of 1.344 Å. The C=N imine bond length is 1.313 Å, within limits of similar compounds.[31] Neutral TCQMI is nearly planar, as noted for Me_3TCQMI.[16a] Interestingly, both the tetramethyl, Me_4TCQMI, and tetramethyl substituted TCNQ, Me_4TCNQ, were deformed into a boat formation.[16a] Important crystallographic parameters of TCQMI, $[FeCp^*_2][TCQMI]$, and $[MnTPP]_2[TCQMI]_2$ are listed in **Table 1**.

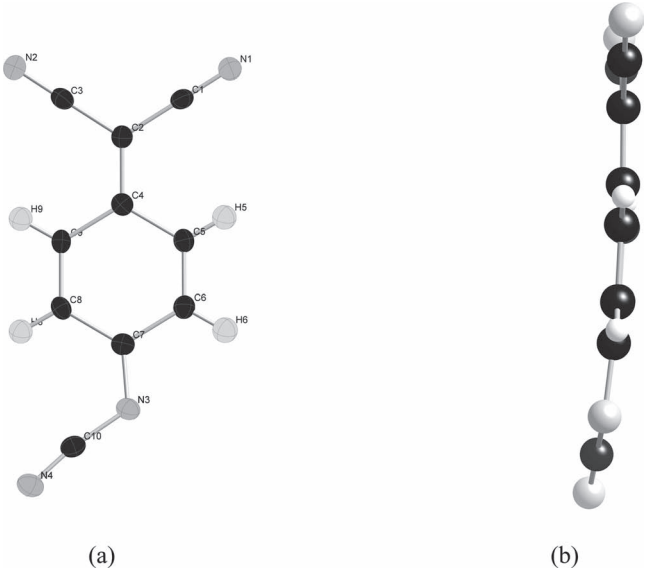

Figure 1. Ortep diagram (50% electron density) of the structure of TCQMI with atom labels (a) and its side view (b) showings its deviation from planarity.

Table 1. Summary of the crystallographic parameters for TCQMI, $[FeCp^*_2][TCQMI]$, and $[MnTPP]_2[TCQMI]_2$.[19]

	TCQMI•½ Benzene	$[FeCp^*_2][TCQMI]$	$[MnTPP][TCQMI]$[19]
molecular formula	$C_{13}H_7N_4$	$C_{30}H_{34}FeN_4$	$C_{54}H_{32}MnN_8$
molecular mass [daltons]	219.23	506.46	847.82
crystal system	Monoclinic	Monoclinic	Monoclinic
space group	$P\,2_1/n$	$P\,2_1$	$P\,2_1/c$
Z	4	2	4
temperature [K]	150(2)	300	100(2)
a [Å]	12.2600(17)	10.5880 (3)	17.6731(15)
b [Å]	6.2948(9)	13.7831 (4)	22.610(2)
c [Å]	14.290(2)	10.7078 (3)	11.5115(9)
α [deg]	90	90	90
β [deg]	100.726(2)	119.644 (4)	107.230(6)
γ [deg]	90	90	90
V [Å^3]	1083.6(3)	1358.13 (8)	4393.5(6)
calcd density [g cm^{-3}]	1.344	1.238	1.282
wavelength [Å]	0.71073	0.699975	1.54178
absorpn coeff [mm^{-1}]	0.086	0.55	2.810
F (000)	452	536	1748
minimum 2θ [deg]	2.01	4.00	3.91
maximum 2θ [deg]	25.41	30.5	63.81
reflections collected	1999	5301	19749
unique reflections	7645		7074
GoF	1.069	2.005	1.048
R_1	0.0408		0.0578
wR_2	0.0971		0.1430
R_{wp}[a,b]		0.0580	
R_{exp}[b,c]		0.0314	

a) $$R_{wp} = \sqrt{\frac{\sum_i w_i (y_i^{calc} - y_i^{obs})^2}{\sum_i w_i (y_i^{obs})^2}}$$

b) y_i^{calc} and y_i^{obs} are the calculated and observed intensities at the i^{th} point in the profile, normalized to monitor intensity. The weight w_i is $1/\sigma^2$ from the counting statistics, with the same normalization factor. N is the number of points in the measured profile minus number of parameters.

c) $$R_{exp} = \sqrt{\frac{N}{\sum_i w_i (y_i^{obs})^2}}$$

The reaction of $Fe^{II}Cp^*_2$ and TCQMI produced microcrystals, which while unsuitable for a single crystal structural determination, were used to obtain high-resolution powder X-ray diffraction data (**Figure 2**). This enabled its structure determination via simulated annealing and Rietveld refinement of the data, and assignment of the composition as $[Fe^{III}Cp^*_2][TCQMI]$ (**Figure 3**). $FeCp^*_2$ was restrained to have identical Fe–C distances that refined to a distance of 2.11(1) Å. The Fe-C_5-ring centroid is 1.744(4) Å. These data are insufficient to distinguish between $Fe^{II}Cp^*_2$ and $[Fe^{III}Cp^*_2]^+$.[32] However, since the IR spectrum indicates that TCQMI is reduced, the composition is $[Fe^{III}Cp^*_2]^+[TCQMI]^{\bullet-}$.

In accord with the IR data indicating that TCQMI is reduced, its structure differs from the TCQMI° (**Table 2**) due to the elongation of C2-C4 by 0.098 Å (7.1%) and C7-N3 by 0.068 (5.2%), and a contraction of C10-N3 by 0.033 Å (2.5%). Additionally, while TCQMI° exhibited a variation in bond lengths for the six-membered ring with alternating single- [1.451(12) Å] and double-bonds [1.344(2) Å]; $[TCQMI]^{\bullet-}$ exhibits a loss of distinct character with C–C ring bonds measuring 1.363(11) and 1.350(17) Å, respectively. Similar behavior is observed for the TCNQ analogue, although the contraction (1.433 to 1.424 Å) and elongation (1.355 to 1.362 Å) are not as dramatic.[33] The same trend is observed for σ-$[TCQMI]_2^{2-}$, with loss of distinct single-bond/double-bond character in the ring, the bonds being much more similar in length. The C–C ring bonds of the dimer are not as uniform as the bonds of the radical anion. This is due to warping of the six-membered ring, although this can also be attributed to steric constants arising from the dimerization, as well as the mode of coordination to the metal centers.

The solid-state motif of $[Fe^{III}Cp^*_2][TCQMI]$ consists of parallel chains possessing alternating $[Fe^{III}Cp^*_2]^{\bullet+}$ and $[TCQMI]^{\bullet-}$, as observed for both $[Fe^{III}Cp^*_2][TCNE]$[4] and $[Fe^{III}Cp^*_2][TCNQ]$.[2] As occurs for $[Fe^{III}Cp^*_2][TCNQ]$, the unit cell contains unique distinct chains with 10.588-Å intrachain Fe•••Fe separations. This motif has three unique pairs of chains (**Figure 4**): out-of-registry **I-III**, **I-IV**, and in-registry **I-II**, and their key interatomic separations are noted in **Figure 5**.

The interchain distances for parallel **I-II**, **I-III**, and **I-IV** chains are 8.52, 9.31, and 8.12 Å, respectively, and have interchain Fe•••Fe separations of 8.524 (**I-II**), 10.707 (**I-III**), and 9.660 and 9.723 (**I-IV**). These distances are comparable to those observed for $[Fe^{III}Cp^*_2][TCNQ]$,[2c] and $[Fe^{III}Cp^*_2][TCNE]$.[34] The intrachain Fe•••N distances measure from 5.849 to 7.121 Å with the shortest distance arising from the imine nitrogen. The interchain Fe•••N distances range from 5.286 to 8.50 Å, with the shorter distances from the imine nitrogen. The interchain N•••N distances range from 3.893 to 7.744 Å. The $[Fe^{III}Cp^*_2][TCQMI]$ chain interactions are intermediate between that observed for $[Fe^{III}Cp^*_2][TCNE]$ and $[Fe^{III}Cp^*_2][TCNQ]$ structures, but span wider ranges due to the cyanimine group.

The $[TCQMI]^{\bullet-}$ is parallel to, and 3.47 Å away from, the Cp^* rings (Figure 3). This structure is very similar to the $[FeCp^*_2]^+$ analogues formed from $[TCNQ]^{\bullet-}$ [2c] and $[TCNE]^{\bullet-}$ [10] where the interplanar separations between the alternating species are 3.56 and 3.52 Å, respectively.

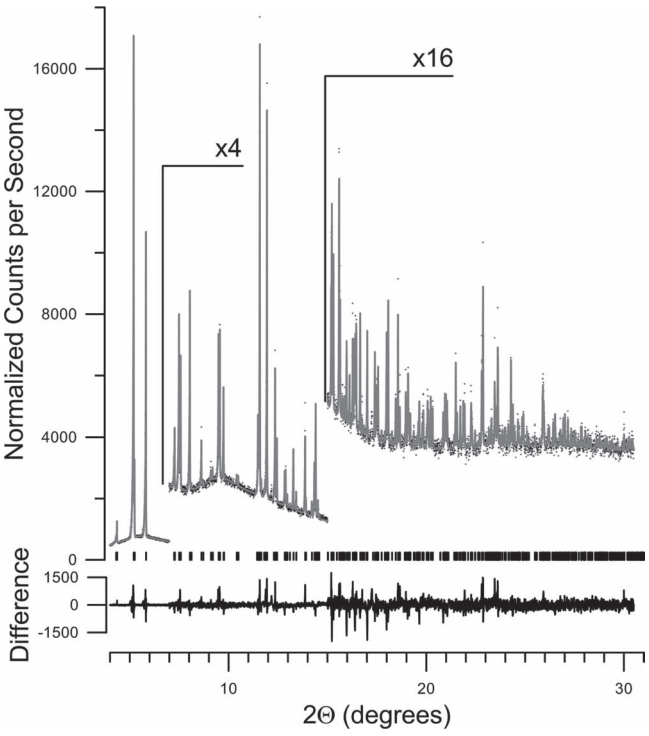

Figure 2. High-resolution synchrotron powder diffraction data (dots) and Rietveld fit of the data for $[Fe^{III}Cp^*_2]^{\bullet+}[TCQMI]^{\bullet-}$ (line). The lower trace is the difference, measured minus calculated, plotted to the same vertical scale.

The reactions of TCQMI with $Fe(CO)_5$ or $V(CO)_6$ formed powders of $M[TCQMI]_2 \bullet zCH_2Cl_2$ (M = Fe, V) composition that were unsuitable for diffraction analysis, as also previously noted from the reaction of TCNQ. $Fe[TCNQ]_2 \bullet zCH_2Cl_2$ and $V[TCNQ]_2 \bullet zCH_2Cl_2$ magnetically ordered at 35[29] and

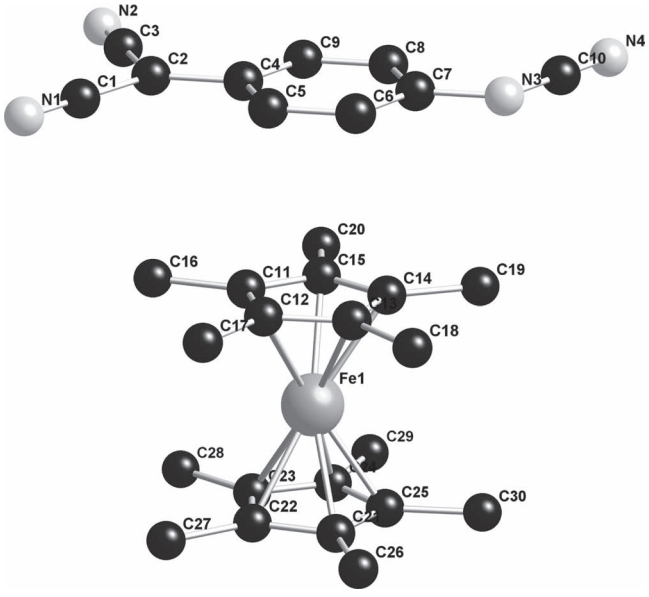

Figure 3. Atom labeling diagram for $[FeCp^*_2][TCQMI]$ (hydrogen atoms not shown for clarity).

Table 2. Comparison of the TCQMI bond distances [Å] with esds observed for TCQMI, Me_3TCQMI,[16a] Me_4TCQMI, [16a] [$Fe^{III}Cp^*_2$][TCQMI], and [MnTPP][TCQMI].[19] Distances marked (a), (b), and (c) were constrained to be equal.

	TCQMI	Me_3TCQMI[16a]	Me_4TCQMI[16a]	[$FeCp^*_2$][TCQMI]	[MnTPP][TCQMI][19]
C2-C4	1.372(2)	1.373(8)	1.360(3)	1.470(25)	1.547(6)
C1-N1	1.149(2)	1.147(5)	1.14(1)	1.142(18) (a)	1.122(5)
C3-N2	1.152(2)	1.144(6)	1.14(2)	1.142(18) (a)	1.135(5)
C4-C5	1.450(2)	1.457(6)	1.47(2)	1.363(11) (b)	1.384(7)
C4-C9	1.451(2)	1.451(4)	1.48(1)	1.363(11) (b)	1.399(5)
C5-C6	1.343(2)	1.360(7)	1.351(4)	1.350(17) (c)	1.382(5)
C8-C9	1.345(2)	1.338(7)	1.354(4)	1.350(17) (c)	1.372(5)
C6-C7	1.452(3)	1.466(4)	1.463(3)	1.363(11) (b)	1.403(5)
C7-C8	1.452(2)	1.462(6)	1.47(1)	1.363(11) (b)	1.398(7)
C7-N3	1.313(2)	1.304(8)	1.299(3)	1.381(23)	1.400(5)
C10-N3	1.345(2)	1.326(4)	1.331(4)	1.312(28)	1.318(4)
C2-C2'	–	–	–	–	1.612(6)

52[22] K, respectively. The ν_{CN} absorptions at 2245, 2173, and 2116 cm^{-1} and 2250 and 2086 cm^{-1}, respectively, for M = Fe and V indicate reduced TCQMI. These stretches are in accord with the ν_{CN} stretches seen in the TCNQ analogues with the same metals.

As previously described, the reaction of Mn^{II}TPP and TCQMI forms reduced TCQMI. Instead of 1D chains of alternating $[Mn^{III}TPP]^+$ and μ-[TCQMI]$^{\bullet-}$, μ_4-σ-$[TCQMI]_2^{2-}$ forms, and possesses a $(NC)_2C–C(CN)_2$ linkage with a long 1.60(1) Å central C–C bond (**Figure 6**).[19] A similar dimerization has

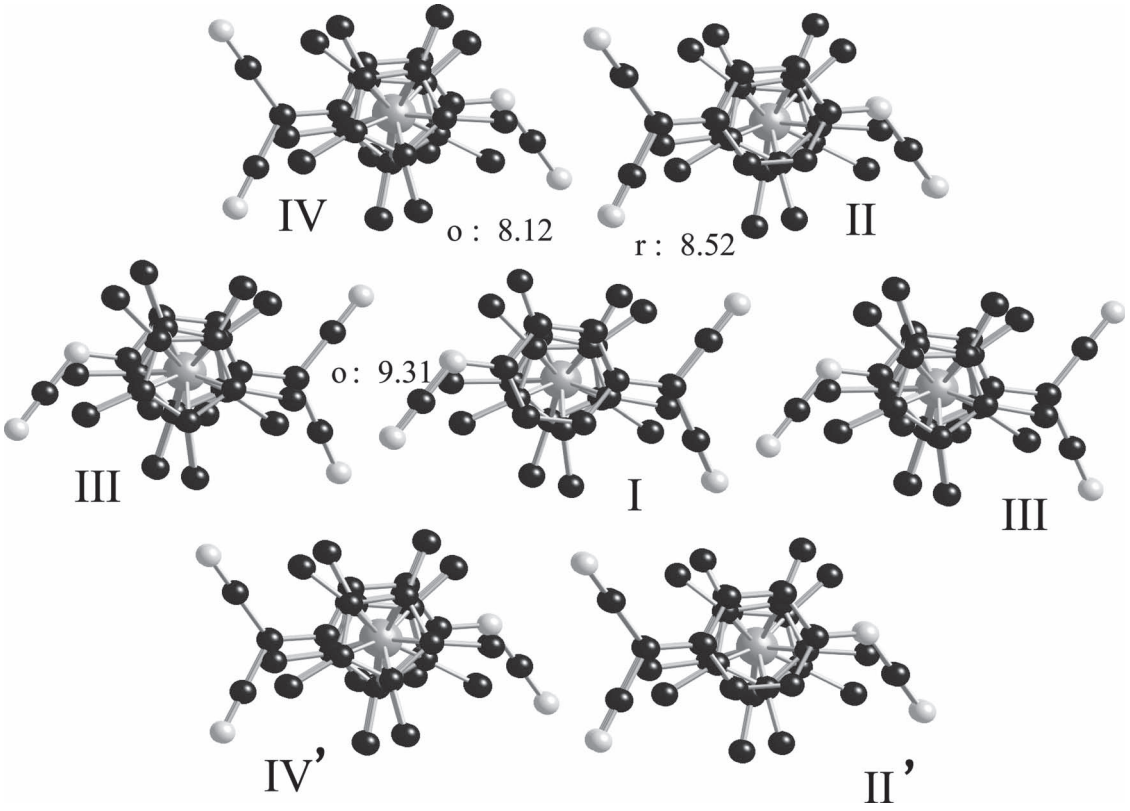

Figure 4. Top-view showing the unique adjacent parallel chains of [$Fe^{III}Cp^*_2$][TCQMI] and their interchain separations (r: in-registry chains; o: out-of-registry chains). Hydrogen atoms not shown for clarity.

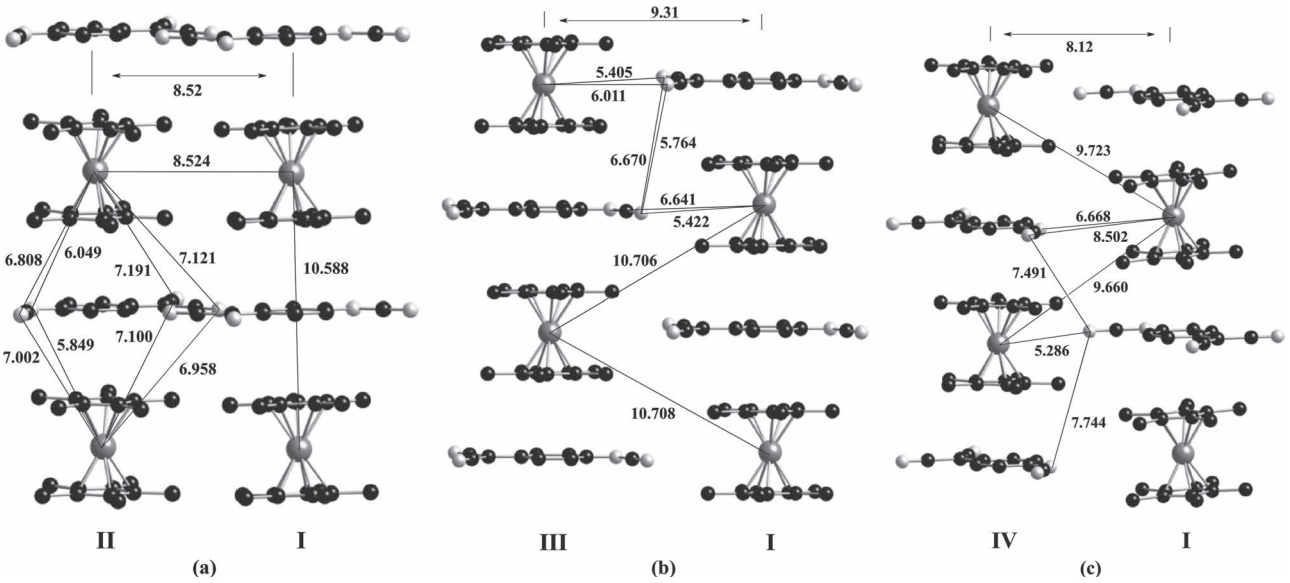

Figure 5. Adjacent in-registry (r) **I-II and** out-of-registry (o) **I-III**, **I-IV** parallel chains of $[Fe^{III}Cp^*_2][TCQMI]$ and their interchain separations. For clarity, hydrogen atoms are not shown.

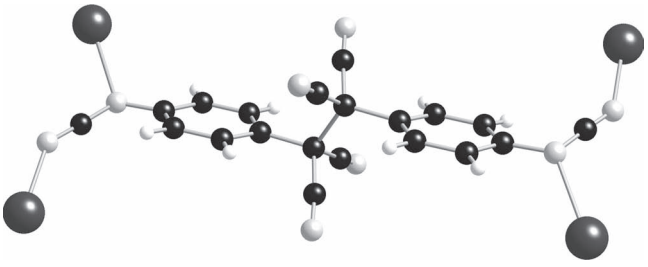

Figure 6. Structure of μ_4-σ-$[TCQMI]_2^{2-}$ present in $[Mn^{III}TPP]_2[TCQMI]_2$.[19]

been noted for TCNE and TCNQ and the central C–C bond length is in accord with related σ-dimers of $[TCNQ]_2^{2-}$ (≈1.6 Å)[35] and $[TCNE]_2^{2-}$ [1.59(2) Å].[13b,36] Mn^{III} ions were bonded by the N–C–N functionality in a $\mu_{1,3}$-bridging manner with Mn-N bond lengths of 2.382 and 2.241 Å. The carbon-nitrogen bond lengths within the NCN fragment (1.318 and 1.161 Å) suggest the structure is best described as a cyanimine (N–C≡N) rather than a carbodiimide (N=C=N) moiety.

In addition to the unusual coordination of the cyanocarbon, the structure of the porphyrin rings was atypical. Considerable warping of the porphyrin plane was noted. The rings adopt a staggered orientation, with adjacent $Mn^{III}TPP$ planes being canted. The overall effect is a 2D honeycomb layered structure with 24-membered rings. This motif is similar to that reported for tetrakis(2,4,6-trimethyphenyl)porphinatomanganese(III) $[TCNQ]^-$ (**1**) that possesses $[TCNQ]_2^{2-}$; however, the porphyrin ring is planar.[35a]

3.2. UV-Vis Measurements

The UV-vis spectra of TCQMI and $[TCQMI]^{\bullet-}$ in MeCN were obtained. $TCQMI^o$ exhibited a peak at 27 500 with shoulders at 25 000 and 28 700 cm^{-1} with a smaller peak at 44 600 cm^{-1}

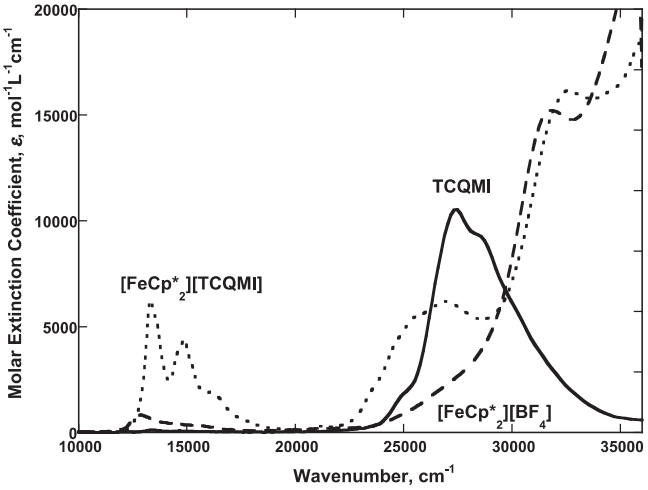

Figure 7. UV-vis spectra of TCQMI (–), $[Fe^{III}Cp^*_2][TCQMI]$ (•••), and $[Fe^{III}Cp^*_2][BF_4]$ (- - -) in MeCN.

(**Figure 7**). $[TCQMI]^{\bullet-}$ has absorption bands at lower energies with respect to $TCQMI^o$. Major peaks occur at 13 300, 14 800, 26 900 and 32 600 cm^{-1}, with shoulders at 13 500, 14 500 and 16 100 cm^{-1}. The general shape and shift seen from the neutral compound to the radical anion are consistent with the spectra for TCNQ and $[TCNQ]^{\bullet-}$.[37] The absorptions around 13 000 cm^{-1} obscure the absorptions for $[FeCp^*_2]^+$ that appears in the region, but bands at 32 450 and 36 100 cm^{-1} identify the cation.

3.3. Magnetic Data

The temperature dependent magnetic susceptibility, $\chi(T)$, data were measured from 2 to 300 K, and are plotted as $\chi T(T)$ and $\chi^{-1}(T)$ for $[FeCp^*_2][TCQMI]$ and $M[TCQMI]_2 \bullet zCH_2Cl_2$ (M = Fe, V) (**Figure 8**).

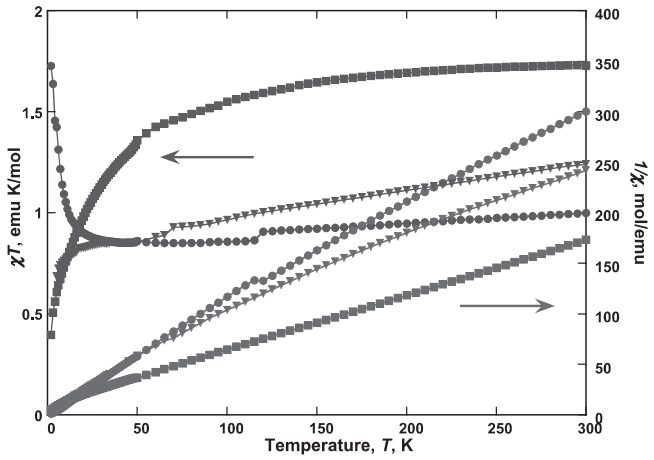

Figure 8. χT (T) and $1/\chi$ (T) for [$FeCp^*_2$][TCQMI] (•), Fe[TCQMI]$_2$ (■), and V[TCQMI]$_2$(▾).

3.3.1. [FeCp*$_2$][TCQMI]

The room-temperature χT value for [$FeCp^*_2$][TCQMI] is 0.995 emu K mol^{-1}, and exceeds the calculated spin-only value of 0.75 emu K mol^{-1} for a system of two $S = 1/2$ ions (Figure 8). This is expected due to the anisotropic nature of [$Fe^{III}Cp^*_2$]$^+$, as has been observed for all [$Fe^{III}Cp^*_2$]$^+$ salts including [$FeCp^*_2$][TCNE][32c] and [$FeCp^*_2$][TCNQ].[4c] The $\chi T(T)$ data can be fit to the Curie-Weiss expression, $\chi \propto (T - \theta)^{-1}$, where θ is the Weiss constant and g is the Lande g-factor, with $\theta = 1.5$ K, and $g = 2.98$. The θ value indicates weak ferromagnetic coupling. The $\chi T(T)$ and $1/\chi(T)$ data show a jump in the data at ≈120 K. This jump occurs in all samples and closer examination of the region indicates this is not an instrumental artifact, but is innate to the system. This jump possibly arises from a phase transition in the compound.

To further investigate the genesis of the small positive θ value, the in-phase (real) and out-of-phase (complex) AC susceptibilities, $\chi'(T)$ and $\chi''(T)$, respectively, were measured between 2 and 10 K, **Figure 9**. $\chi'(T)$ exhibits a frequency independent peak at 3.4 K, and a frequency dependent upturn in $\chi''(T)$ with decreasing temperature. This indicates that more complicated magnetic ordering occurs with a T_c of 3.4 K. Interestingly, the AC susceptibility data was seen to be identical whether the solution was taken to dryness or precipitated in a freezer.

Saturation of the magnetization, M_s, is achieved at ≈50 kOe at 2 K, and is 2700 emu K mol^{-1}. This value is much lower than that seen for the TCNE and TCNQ analogues[4c] and the calculated M_s value expected for a ferromagnetically ordered system, i.e., 13 900 emu K mol^{-1} assuming the aforementioned $g = 2.98$. The value is consistent with an antiferromagnetically coupled ferrimagnetically ordered system, i.e., 2736 emu K mol^{-1} as calculated from $M_s = N\Delta gS\mu_B$ where N = Avogadro's number and μ_B is the Bohr magneton. Ferrimagnets arise from antiferromagnetic coupling whereby the antiparallel spins cannot cancel due to different g-values. The behavior is still anomalous as hysteresis was not evident from a 2-K (± 90 kOe) $M(H)$ study.

3.3.2. Fe^{II}[TCQMI]$_2$•zCH_2Cl_2

The room-temperature χT value for Fe^{II}[TCQMI]$_2$•zCH_2Cl_2 is 1.62 emu K mol^{-1}, and it substantially reduced the calculated spin-only value of 2.75 emu K mol^{-1} for a system of two $S = 1/2$ ions plus an $S = 2$ high-spin Fe^{II} ion (Figure 8). This must arise for antiferromagnetic coupling. The $\chi T(T)$ data can be fit to the data to the Curie-Weiss expression with $\theta = -14$ K indicating antiferromagnetic coupling.

The 2 to 10 K $\chi'(T)$ and $\chi''(T)$ AC susceptibilities exhibit a frequency dependent peak in $\chi'(T)$ at 3.7 K at 1000 Hz, and onset at 4.4 K upon cooling for $\chi''(T)$, **Figure 10**. Hence, magnetic ordering occurs ≈4 K substantially reduced from that observed for Fe[TCNE]$_2$ (T_c ≈ 100 K) and Fe[TCNQ]$_2$ (T_c ≈ 35 K).[29] The frequency dependent data suggest spin glass behavior. Similar behavior is observed in the heat-annealed Fe[TCNQ]$_2$, which is also classified as a spin-glass. However, Fe[TCNQ]$_2$ exhibits a bifurcation in the zero-field-cooled and field-cooled (ZFC/FC) magnetization data, while Fe^{II}[TCQMI]$_2$•zCH_2Cl_2 does not indicate bifurcation.[29] The magnetization is 5800 emu K mol^{-1} at 90 kOe at 2 K, but it is still increasing with increasing applied field, and thus is not saturated. The low value suggests a weak ferromagnetic behavior. Hysteresis was not evident from a 2-K (± 90 kOe) $M(H)$ study.

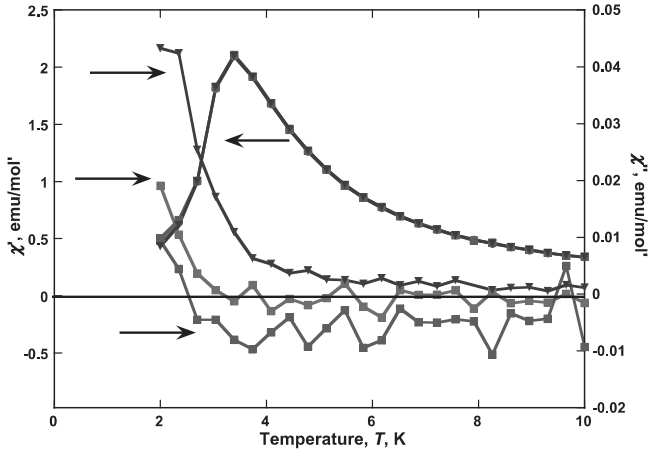

Figure 9. Frequency dependency of $\chi'(T)$ and $\chi''(T)$ for [$FeCp^*_2$][TCQMI] (33 Hz: •), 100 Hz: (■), 1000 Hz: (▾).

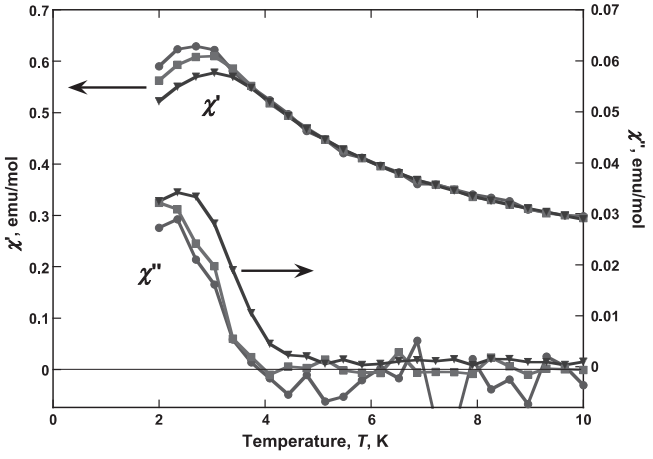

Figure 10. Frequency dependency of $\chi'(T)$ and $\chi''(T)$ for Fe[TCQMI]$_2$•0.40CH_2Cl_2 (33 Hz: •), 100 Hz: (■), 1000 Hz: (▾).

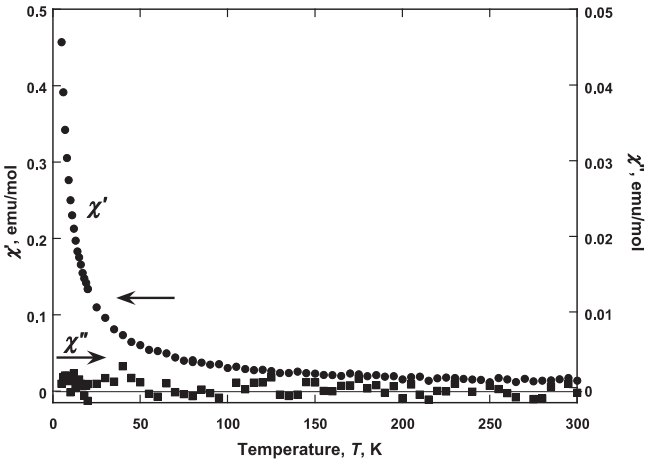

Figure 11. 1000-Hz $\chi'(T)$ (•) and $\chi''(T)$ (■) for $V[TCQMI]_2 \bullet 0.10CH_2Cl_2$.

3.3.3. $V^{II}[TCQMI]_2 \bullet zCH_2Cl_2$

The room-temperature χT value for $V[TCQMI]_2$ is 0.88 emu K mol^{-1} (Figure 8), well below the value of 1.59 emu K mol^{-1} reported for $V[TCNQ]_2 \bullet zCH_2Cl_2$ with $S = 3/2$ V^{II} and two $S = 1/2$ radical anions. $\chi T(T)$ linearly decreases with decreasing temperature, but has no evidence of magnetic ordering. The $1/\chi(T)$ data indicated antiferromagnetic ordering with a $\theta = -1.8$ K. This is also noted from 1000-Hz 2 to 10 K $\chi''(T)$ data that did have an absorption (**Figure 11**). $\chi'(T)$ increases with decreasing temperature suggesting a peak and perhaps ordering below 2 K. The reason for the lack of ordering in the magnetic phase is not currently understood, as TCQMI forms magnetically ordered compounds in the reaction with other metal systems.[19]

4. Conclusion

The structures and electron accepting properties of cyanocarbon *N*,7,7-tricyanoquinomethanimine, TCQMI, its radical anion $[TCQMI]^{\bullet-}$, and its σ-dimer, σ-$[TCQMI]_2^{2-}$, are reported. The close similarity between the reduction potential of TCQMI (0.20 V vs. SCE), TCNE, and TCNQ, as well as their structures suggest TCQMI as a candidate in forming new molecule-based materials. Additionally, it was expected to form compounds of $M^{II}[TCQMI]_2$ stoichiometry with all nitriles bonded, resulting in less disorder structures. This was studied through the synthesis and characterization of a new series of TCQMI-based magnetic materials from reactions of TCQMI with decamethylferrocene ($FeCp^*_2$), iron pentacarbonyl, vanadium hexacarbonyl, and pyridine tetraphenylporphinatomanganese(II), $Mn^{II}(TPP)(py)$.

The reaction of $[FeCp^*_2]^+[TCQMI]^{\bullet-}$ showed a close correlation with other cyanocarbon acceptors, e.g., TCNE and TCNQ, as it formed a motif composed of 1D, parallel chains of alternating $[Fe^{III}Cp^*_2]^{\bullet+}$ and $[TCQMI]^{\bullet-}$ ions. The inter- and intrachain separations are comparable to those reported for $[FeCp^*_2][TCNE]$ and $[FeCp^*_2][TCNQ]$. $[Fe^{III}Cp^*_2]^{\bullet+}$ and [TCQMI] magnetically orders at a T_c of 3.4 K, intermediate of that reported for $[FeCp^*_2][TCNE]$ and $[FeCp^*_2][TCNQ]$.

$M[TCQMI]_2 \bullet zCH_2Cl_2$ does not order for M = V, but for M = Fe it orders at a low temperature of 3.7 K, in contrast to the significantly higher ordering temperatures for $M[TCNE]_2 \bullet zCH_2Cl_2$ and $M[TCNQ]_2 \bullet zCH_2Cl_2$ (M = V, Fe). The source of the low ordering in $Fe[TCQMI]_2$ and lack of ordering in $V[TCQMI]_2$ is not currently understood.

Acknowledgements

The authors appreciate the continued partial support by the Department of Energy Division of Material Science (Grant No. DE-FG03-93ER45504). Use of the National Synchrotron Light Source, Brookhaven National Laboratory, was supported by the U.S. Department of Energy, Office of Basic Energy Sciences, under Contract No. DE-AC02-98CH10886.

Received: August 17, 2011
Revised: October 7, 2011
Published online: March 14, 2012

[1] a) J. Ferraris, D. O. Cowan, V. Walatka, J. H. Perlstein, *J. Am. Chem. Soc.* **1973**, *95*, 948; b) A. Bright, A. F. Garito, A. J. Heeger, *Solid State Commun.* **1973**, *13*, 943; c) M. J. Cohen, L. B. Coleman, A. F. Garito, A. J. Heeler, *Phys. Rev. B* **1974**, *10*, 1298.
[2] a) G. A. Candela, L. J. Swartzendruber, J. S. Miller, M. J. Rice, *J. Am. Chem. Soc.* **1979**, *101*, 2755; b) J. S. Miller, A. H. Reis Jr., E. Gerbert, J. J. Ritsko, W. R. Saleneck, L. Kovnat, T. W. Cape, R. P. Van Duyne, *J. Am. Chem. Soc.* **1979**, *101*, 7111; c) J. S. Miller, J. H. Zhang, W. M. Reiff, L. D. Preston, A. H. Reis Jr., E. Gerbert, M. Extine, J. Troup, M. D. Ward, *J. Phys. Chem.* **1987**, *91*, 4344.
[3] M. L. Taliaferro, F. Palacio, J. S. Miller, *J. Mater. Chem.* **2006**, *16*, 2677.
[4] a) J. S. Miller, J. C. Calabrese, A. J. Epstein, R. W. Bigelow, J. H. Zhang, W. M. Reiff, *J. Chem. Soc. Chem. Commun.* **1986**, 1026; b) J. S. Miller, A. J. Epstein, W. M. Reiff, *Science.* **1988**, *240*, 40; c) J. S. Miller, A. J. Epstein, W. M. Reiff, *Chem. Rev.* **1988**, *88*, 201; d) J. S. Miller, A. J. Epstein, W. M. Reiff, *Acc. Chem. Res.* **1988**, *21*, 114.
[5] J. S. Miller, J. C. Calabrese, R. L. Harlow, D. A. Dixon, J. H. Zhang, W. M. Reiff, S. Chittipeddi, C. Mark, A. Selover, A. J. Epstein, *J. Am. Chem. Soc.* **1990**, *112*, 5496.
[6] a) J. S. Miller, *Inorg. Chem.* **2000**, *39*, 4392; b) J. Zhang, P. Zhou, W. B. Brinckerhoff, A. J. Epstein, C. Vazquez, R. S. McLean, J. S. Miller, *ACS Symp. Ser.* **1996**, *644*, 311; c) J. Zhang, J. Ensling, V. Ksenofontov, P. Gütlich, A. J. Epstein, J. S. Miller, *Angew. Chem. Int. Ed.* **1998**, *37*, 657; d) H. Matsuura, K. Miyake, H. Fukuyama, *J. Phys. Soc. Jpn.* **2010**, *79*, 034712.
[7] a) K.-i. Sugiura, S. Mikami, M. T. Johnson, J. W. Raebiger, J. S. Miller, K. Iwasaki, Y. Okada, S. Hino, Y. Sakata, *J. Mater. Chem.* **2001**, *11*, 2152; b) H. -P. Werner, J. U. Von Schütz, H. C. Wolf, R. Kremer, M. Gehrke, A. Aumüller, P. Erk, S. Hünig, *Solid State Commun.* **1988**, *65*, 809.
[8] J. Tanaka, C. Katayama, H. Kumagai, G. Saito, T. Enoki, H. Inokuchi, *Mol. Cryst. Liq. Cryst.* **1985**, *125*, 223.
[9] D. O'Hare, A. Rai-Chaudhuri, V. Murphy, *J. Chem. Soc., Dalton Trans.* **1993**, *20*, 3071.
[10] J. S. Miller, *J. Mater. Chem.* **2010**, *20*, 184
[11] a) S. J. Blundell, F. L. Pratt, *J. Phys.: Condens. Matter* **2004**, *16*, R771; b) V. I. Ovcharenko, R. Z. Sagdeev, *Russ. Chem. Rev.* **1999**, *68*, 345; c) J. S. Miller, A. J. Epstein, *Chem. Commun.* **1998**, 1319; d) J. S. Miller, A. J. Epstein, *Angew. Chem. Int. Ed. Engl.* **1994**, *33*, 385.
[12] K. H. Stone, P. W. Stephens, A. C. McConnell, E. Shurdha, K. I. Pokhodnya, J. S. Miller, *Adv. Mater.* **2010**, *22*, 2514.

[13] a) K. I. Pokhodnya, M. Bonner, J. H. Her, P. W. Stephens, J. S. Miller, *J. Am. Chem. Soc.* **2006**, *128*, 15592; b) J. H. Her, P. W. Stephens, K. I. Pokhodnya, M. Bonner, J. S. Miller, *Angew. Chem. Int. Ed.* **2007**, *46*, 1521; c) S. H. Lapidus, A. C. McConnell, P. W. Stephens, J. S. Miller, *Chem. Commun.* **2011**, *47*, 7602.
[14] R. Clerac, S. O'Kane, J. Cowen, X. Ouyang, R. Heintz, H. Zhao, J. J. Bazile Jr., K. R. Dunbar, *Chem. Mater* **2003**, *15*, 1840.
[15] a) L. Shields, *J. Chem. Soc., Faraday Trans 2* **1985**, *81*, 1; b) R. A. Heintz, H. Zhao, X. Ouyang, G. Grandinetti, J. Cowen, K. R. Dunbar, *Inorg. Chem.* **1999**, *38*, 144.
[16] a) M. R. Bryce, S. R. Davies, A. M. Grainger, M. B. Hursthouse, M. Mazid, R. Bachmann, F. Gerson, J. Hellberg, *J. Org. Chem.* **1992**, *57*, 1690; b) J. A. Hyatt, *J. Org. Chem.* **1983**, *48*, 129; c) S. Iwatsuki, T. T. Itoh, H. Itoh, *Chem. Lett.* **1988**, *17*, 1187.
[17] J. S. Miller, J. L. Manson, *Acc. Chem. Res.* **2001**, *34*, 563.
[18] B. Olbrich-Deussner, W. Kaim, R. Gross-Lannert, *Inorg. Chem.* **1989**, *28*, 3113.
[19] J. L. Arthur, C. E. Moore, A. L. Rheingold, J. S. Miller, *Inorg. Chem.* **2011**, *50*, 2735.
[20] X. Liu, J. E. Ellis, T. D. Selby, P. Ghalsasi, J. S. Miller, *Inorg. Synth.* **2004**, *34*, 68.
[21] J. Attenburrow, A. F. B. Cameron, J. H. Chapman, R. M. Evans, B. A. Hems, A. B. A. Jansen, T. Walker, *J. Chem. Soc.* **1952**, 1094.
[22] E. B. Vickers, T. D. Selby, M. S. Thorum, M. L. Taliaferro, J. S. Miller, *Inorg. Chem.* **2004**, *43*, 6414.
[23] E. J. Brandon, D. K. Rittenberg, A. M. Arif, J. S. Miller, *Inorg. Chem.* **1998**, *37*, 3376.
[24] a) Saint Plus, v. 6.02; *Bruker Analytical X-ray*: Madison, WI **1999**; b) G. M. Sheldrick, *SADABS*; University of Göttingen: Göttingen, Germany **1996**.
[25] a) I. Goldberg, H. Krupitsky, Z. Stein, Y. Hsiou, C. E. Strouse, *Supramol. Chem* **1995**, *4*, 203; b) H. Krupitsky, Z. Stein, I. Goldberg, *J. Inclusion Phenom. Mol. Recognit. Chem.* **1995**, *20*, 211; c) I. Goldberg, *Mol. Cryst. Liq. Cryst.* **1996**, *278*, 767; d) M. P. Byrn, C. J. Curtis, Y. Hsiou, S. I. Kahn, P. A. Sawin, S. K. Tendick, A. Terzis, C. E. Strouse, *J. Am. Chem. Soc.* **1993**, *115*, 9480; e) M. P. Byrn, C. J. Curtis, Y. Hsiou, S. I. Khan, P. A. Sawin, A. Terzis, C. E. Strouse, in *Comprehensive Supramolecular Chemistry Vol. 6* (Eds: J. L. Atwood, J. E. D. Davies, D. D. MacNicol, F. Vogtle), Pergamon, New York **1996**, p 715.
[26] A. A. Coelho, *J. Appl. Cryst.* **2003**, *36*, 86.
[27] A. A. Coelho, TOPAS Academic, available at www.topas-academic.net (accessed January 2012).
[28] K. Nakamoto, in *Infrared and Raman Spectra of Inorganic and Coordination Compounds*, Wiley-Interscience, New York **1997**, p. 111.
[29] K. I. Pokhodnya, N. Petersen, J. S. Miller, *Inorg. Chem.* **2002**, *41*, 1996.
[30] A. Aumüller, E. Peter, S. Hünig, H. Meixner, J.-U. von Schütz, H.-P. Werner, *Liebigs Ann. Chem.* **1987**, 997.
[31] A. Aumüller, P. Erk, S. Hünig, H. G. von Schnering, *Chem. Ber.* **1991**, *124*, 2001.
[32] a) J. S. Miller, D. T. Glatzhofer, C. Vazquez, R. S. McLean, J. C. Calabrese, W. J. Marshall, J. W. Raebiger, *Inorg. Chem.* **2001**, *40*, 2058; b) B. Bildstein, A. Hradsky, H. Kopacka, R. Malleier, K.-H. Ongania, *J. Organomet. Chem.* **1997**, *540*, 127; c) J. S. Miller, J. C. Calabrese, H. Rommelmann, S. Chittipeddi, A. J. Epstein, J. H. Zhang, W. M. Reiff, *J. Am. Chem. Soc.* **1987**, *109*, 769; d) D. P. Freyberg, J. L. Robbins, K. N. Raymond, J. C. Smart, *J. Am. Chem. Soc.* **1979**, *101*, 892.
[33] V. A. Nadtochenko, N. N. Denisov, I. V. Rubtsov, A. S. Lobach, A. P. Moravskii, *Chem. Phys. Lett.* **1993**, *208*, 431.
[34] a) J.-H. Her, P. W. Stephens, J. Ribas-Ariño, J. J. Novoa, W. W. Shum, J. S. Miller, *Inorg. Chem.* **2009**, *48*, 3296; b) J. S. Miller, P. K. Gantzel, A. L. Rheingold, M. L. Taliaferro, *Inorg. Chem.* **2009**, *48*, 4201.
[35] a) S. Mikami, K.-i. Sugiura, J. S. Miller, Y. Skata, *Chem Lett.* **1999**, *28*, 413; b) H. Zhao, R. A. Heinz, K. R. Dunbar, R. D. Rogers, *J. Am. Chem. Soc.* **1996**, *118*, 12844; c) R. H. Harms, H. J. Keller, D. Nöthe, M. Werner, D. Grundel, H. Sixl, Z. G. Soos, R. M. Metzger, *Mol. Cryst. Liq. Cryst.* **1981**, *65*, 179; d) S. K. Hoffman, P. J. Corvan, P. Singh, C. N. Sethuklekshmi, R. M. Metzer, W. E. Hatfield, *J. Am. Chem. Soc.* **1983**, *105*, 4608; e) V. Dong, H. Endres, H. J. Keller, W. Moroni, D. Nöthe, *Acta Crystallogr.* **1977**, *B33*, 2428.
[36] a) J. Zhang, L. M. Liable-Sands, A. R. Rheingold, R. E. Del Sesto, D. C. Gordon, B. M. Burkhart, J. S. Miller, *Chem. Commun.* **1998**, 1385; b) J. S. Miller, *Angew. Chem. Int. Ed.* **2006**, *45*, 2508; *Angew. Chem.* **2006**, *118*, 2570; c) K. I. Pokhodnya, M. Bonner, A. G. DiPasquale, A. L. Rheingold, J. S. Miller, *Chem. -Eur. J.* **2008**, *14*, 714; d) K. I. Pokhodnya, M. Bonner, A. G. DiPasquale, A. L. Rheingold, J. S. Miller, *Angew. Chem.* **2007**, *119*, 1543.
[37] L. R. Melby, R. J. Harder, W. R. Hertler, W. Mahler, R. E. Benson, W. E. Mochel, *J. Am. Chem. Soc.* **1962**, *84*, 3374.